

Preparation and Antibacterial Properties of Poly(N-hydroxymethyl Acrylamide)/Na-montmorillonite Composites via *in situ* Polymerization

Sibel Erol Dağ¹, Pınar Acar Bozkurt², Nurcan Acar², Leyla Açık³ and Meltem Çelik^{2*}

¹Ankara University, Graduate School of Natural and Applied Sciences, 06100 Beşevler, Ankara, Turkey

²Ankara University, Department of Chemistry, Faculty of Science, 06100 Tandoğan, Ankara, Turkey

³Gazi University, Department of Biology, Faculty of Science, 06500 Teknikokullar, Ankara, Turkey

*Corresponding author (e-mail: mecelik@science.ankara.edu.tr)

In the present study, poly(N-hydroxymethyl acrylamide) (PHMAm)/unmodified Na-montmorillonite (Na-MMT) composites had been successfully synthesized by *in situ* radical polymerization and the antibacterial activities of the composites against Gram (+) and Gram (-) bacteria were scrutinized. The structure, morphology, and particle size of prepared composites were characterized by Fourier infrared spectroscopy, X-ray diffraction (XRD), scanning electron microscopy (SEM), and transmission electron microscopy (TEM). According to the XRD analysis, the interlayer spacing of montmorillonite layers was expanded. SEM images showed that the morphology of composites was spongy and porous cauliflower-like shape. TEM revealed the Na-montmorillonite intercalated in poly(N-hydroxymethyl acrylamide) matrix. All the obtained composites exhibited good antibacterial activity against various pathogens bacterial strain particularly *Pseudomonas aeruginosa* Gram (-) using disk diffusion method. The antibacterial activity of composites was increased with HMAm monomer content except *Escherichia coli* 35218.

Key words: Composite; Na-montmorillonite; poly(N-hydroxymethyl acrylamide); benzoyl peroxide; *in situ* polymerization

Received: November 2017; Accepted: June 2018

In recent years, polymer/clay composites have attracted considerable attention due to their remarkable properties such as enhanced mechanical properties, thermal stability, gas-barrier, and antibacterial properties compared to pure polymer [1-6]. Among its properties, the antibacterial property of polymer/clay composites is the most important feature to use for antibacterial applications since eco-friendly materials. In addition, polymer/clay composites with antibacterial activity have been received as a new class of biomedical materials.

The inorganic layered material clays are relatively low cost, abundant, and have excellent

chemical and thermal resistance for synthesis polymer/clay composite. Among the many-layered materials, the Na-montmorillonite (Na-MMT) is one of the widely used inorganic materials for this purpose and consists of layers of two tetrahedral silica sheets sandwiching one octahedral alumina sheet [7, 8]. It has intercalation and exfoliation characteristics. With only a low content of MMT, improved physical properties of the polymer can be obtained. In addition, the hydrophilic nature of the clay surfaces provides homogeneous dispersion in the organic polymer phase [9]. Use of clay minerals as inorganic fillers also reduce the cost of inorganic/organic composite products.

N-hydroxymethyl acrylamide (HMAM) is one of most important monomers for acting as a crosslinking agent in some emulsion polymerization systems and it is very easy to polymerize because of the hydrophilic nature of the HMAM [10]. Also, poly(*N*-hydroxymethyl acrylamide) (PHMAM) is biodegradable and biocompatible. It is a hydrophilic and nonionic polymer with hydroxyl groups on the side chain covering a hydrophobic carbon-carbon backbone. It is widely used for many applications such as protective coatings and textile binders. However, the poor thermal and mechanical properties especially thermal stability, and also antibacterial properties need to be improved.

There are many studies for the preparation of polymer/clay composites in the literature, there is little work on preparation, characterization and antibacterial properties of poly(*N*-hydroxymethyl acrylamide)/unmodified Na-montmorillonite composites synthesized by *in situ* polymerization.

Owing to our interest in developing new materials with improved properties, the purpose of this study was to improve the antibacterial activities the prepared composites against various strains via PHMAM through the synthesis and modify with layered materials such as clay.

EXPERIMENTAL

Materials

All chemicals were purchased from Merck (Germany). A free radical initiator, benzoyl peroxide (Bz_2O_2) (Merck) was twice purified by recrystallization from methanol and chloroform mixture.

Reagent grade *N*-hydroxymethyl acryla-

mid (HMAM) (Merck) monomer was used without further purification. The clay used in this study was Na-montmorillonite (Na-MMT) provided by Reşadiye (Tokat/Turkey) and was used after further purification [9]. Its specific surface is $67.56 \text{ m}^2/\text{g}$, and its XRD analysis shows that the interlayer spacing of Na-MMT is 1.18 nm. All the bacterial strains were obtained from the Department of Biology, Gazi University of Ankara, Turkey. All other chemicals were of analytical reagent grade and used without further purification.

Synthesis of PHMAM/Na-MMT Composites

Na-montmorillonite was obtained, as previously described in the literature by the methods of dispersion and sedimentation from its aqueous suspension [11]. The PHMAM/Na-MMT composites were synthesized using *in situ* free radical polymerization of HMAM monomer in aqueous medium [12,13].

In this synthesis procedure, 1 g Na-montmorillonite was dispersed in 24 ml of distilled water in a 100 ml Pyrex glass tube and the obtained dispersion was stirred at a rate of 100 rpm in overnight at room temperature for each polymerization. The HMAM and the aqueous Na-MMT suspension were mixed with the different weight ratios as given in Table 1. By the addition of the solution of Bz_2O_2 in 1 ml acetone ($3.59 \times 10^{-3} \text{ mol/l}$), the mixture was polymerized in an ultrasonic bath (Bandelin Sonalex RK 100H, Germany) at 85°C for 2 h to synthesize the PHMAM/Na-MMT composites. Finally, the obtained composites were left dry in a vacuum oven at 30°C and weighed. The same procedure was adopted for other samples using different quantities of HMAM.

Table 1. Preparation conditions of PHMAM/Na-MMT composites^a.

Sample code	Monomer content (wt%)
PHMAM/Na-MMT-1	33.33
PHMAM/Na-MMT-2	50.00
PHMAM/Na-MMT-3	71.43
PHMAM/Na-MMT-4	80.00

PHMAM: poly(*N*-hydroxymethyl acrylamide); MMT: montmorillonite.
^a $[Bz_2O_2]$: $3.59 \times 10^{-3} \text{ mol/l}$, temperature: 85°C , time: 2 h.

Characterization of PHMAm/Na-MMT Composites

Fourier transform infrared (FTIR) spectra were recorded in KBr pellets by a Bruker IFS 66/S Model FTIR spectrophotometer in the range 400-4000 cm^{-1} .

The XRD patterns of Na-MMT and PHMAm/Na-MMT composites in powder form were recorded using a Rigaku D/MAX 2200 X-ray diffractometer. Composites were analyzed in a 2θ range of 2-40°, at the scanning speed of 0.15°/min using $\text{CuK}\alpha$ radiation ($\lambda = 1.5418 \text{ \AA}$).

Scanning electron microscopy was applied to observe surface morphology of pure Na-montmorillonite and composites using a Quanta 400F Field Emission instrument. The surface of all samples was coated by thin layer gold prior to analysis.

The microstructure of composites was observed using a TEM-FEIN, model Tecnai G2 F30 transmission electron microscope (TEM) with at an accelerating voltage of 120 kV. The samples cured epoxy resin was microtomed with a Leica ultracut-R. Ultrathin sections were cut with a glass knife and deposited on one layer of carbon 300 mesh copper grids prior to analysis.

The antibacterial activity of prepared PHMAm/Na-MMT composites was verified by *in vitro* different bacterial species. *Bacillus cereus* G (+), *Staphylococcus aureus* G (+), *Proteus vulgaris* G (-), *Pseudomonas aeruginosa* G (-), and *Escherichia coli* (35218) G (-) were used to evaluate the antibacterial activity by disc diffusion method [4,14-16]. This method is a means of measuring the efficiency of an antibacterial agent against the bacterial growth. In this method: Composites were cut to make 16 mm in diameter for measurement of antibacterial activity. Inoculums of bacteria were prepared in 0.85% saline using McFarland standard and inoculated uniformly on nutrient agar plates. The disc was placed on the agar surface of the plate. The zone of inhibition for each composite was measured after overnight incubation at 37°C. If the bacteria are susceptible to a particular compound, an area of clearing surrounds the wafer where bacteria are not capable of growing (called a zone of inhibition).

The size of the zone of inhibition shows the antibacterial activity was ordered as strong activity (> 13mm), moderate activity (6-12mm), weak activity (5mm) or no activity (inhibition zone < 5mm) [17].

RESULTS AND DISCUSSION

FTIR Analysis

The FTIR spectrum of PHMAm/Na-MMT-4 composite as depicted in Figure 1 shows the characteristic peaks of appeared from 400-4000 cm^{-1} range. In the FTIR spectrum of composite, the characteristic peaks of PHMAm at 3292 cm^{-1} as broad single peak (N-H stretching), 1650 cm^{-1} (CO amide) and 1530 cm^{-1} (C-N) resonance; and the characteristic peaks of Na-MMT at 3630 cm^{-1} (O-H stretching), 470 cm^{-1} (Mg-O), 1040 cm^{-1} and 515 cm^{-1} (Al-O-Si) is also observed. This spectrum indicates the interaction between Na-MMT and polymer matrix. The peaks have been identified consistent with the prior published literature [18, 19].

Confirmation of intercalation by XRD analysis. XRD analysis was utilized to confirm the existence and formation of Na-MMT in PHMAm. The patterns of the Na-MMT and PHMAm/Na-MMT composites are shown in Figure 2(a-c). In Na-MMT, the peak at $2\theta = 7.46^\circ$ corresponds to d_{001} interlayer spacing (1.18 nm) [4, 6]. The interlayer spacing values (d_{001}) of the samples is found by using Bragg's law ($d = n\lambda/2\sin\theta$, with $\lambda = 1.5418 \text{ \AA}$). The XRD patterns of the PHMAm/Na-MMT-2 and PHMAm/Na-MMT-4 revealed a broad peak at composites showed that the characteristic crystalline peak was shifted toward smaller angles, consequently, increase in the interlayer spacing. This confirmed the intercalation of PHMAm chains between the layers of Na-MMT [Figure 2 (b and c)]. The interlayer spacing was calculated to be 1.97 nm for PHMAm/Na-MMT-2 while in case of PHMAm/Na-MMT-4 it was noticed to be 1.95 nm. An increase of approximately 0.79 nm expansion in the d-spacing value demonstrates that the PHMAm molecules are intercalated into the interlayer space of clay. These results indicate and supported that the PHMAm molecules penetrate through the galleries of clay and expanding the interlayer spacing. This is direct

evidence that intercalated PHMAm/Na-MMT
composites have been synthesized. Similar

behavior has been reported in the literature by
many other researchers [19-21].

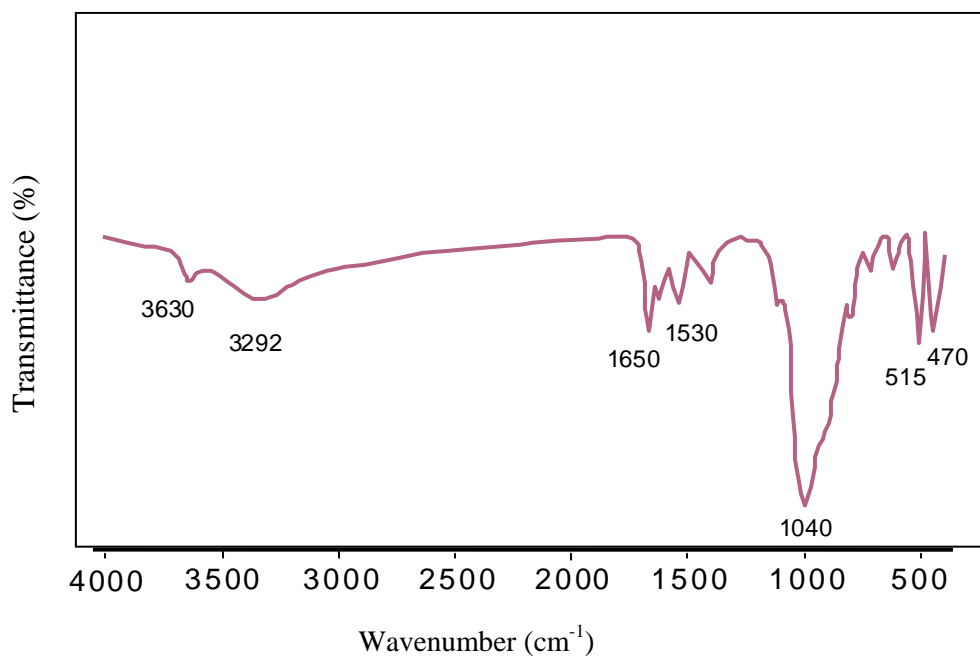


Figure 1. FTIR spectrum of PHMAm/Na-MMT-4 composite.

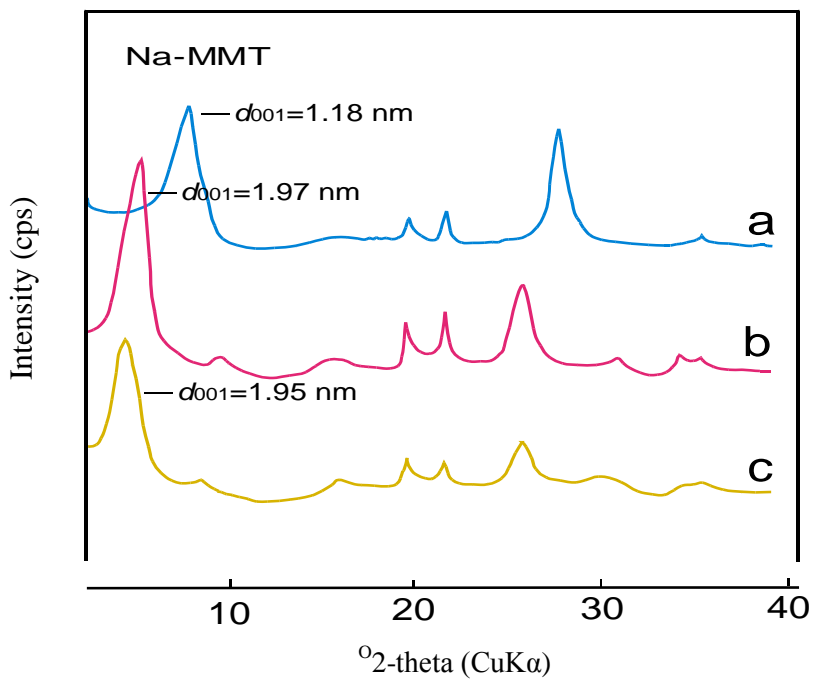
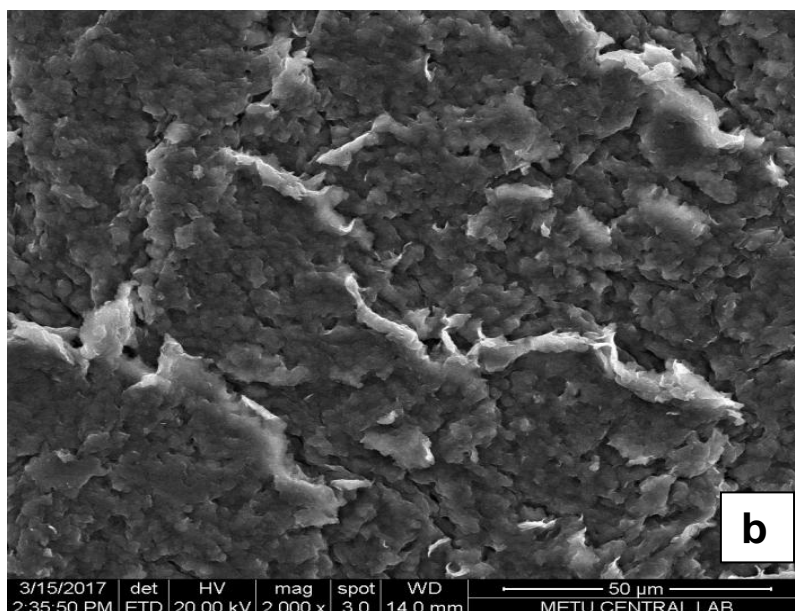
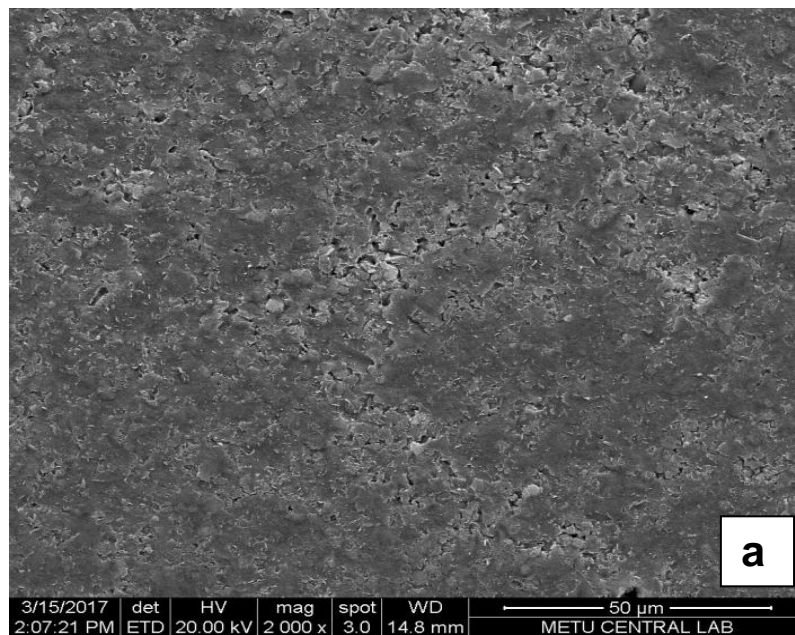


Figure 2. XRD patterns of (a) Na-MMT, (b) PHMAm/Na-MMT-2 composite, and (c) PHMAm/Na-MMT-4 composite.

Scanning electron microscopy analysis of composites. The surface morphologies of Na-MMT and PHMAM/Na-MMT composites and also the distribution of the Na-MMT layers in the polymer matrix were examined by SEM. As shown in Figure 3(a), Na-MMT exhibited an aggregated and sheet-like plates structure before the intercalation. After Na-MMT was intercalated with PHMAM, the significant changes in morphology as illustrated in Figure 3(b) and (c). It

can be seen that PHMAM polymerization occurred within the Na-MMT layers and a satisfactory dispersion of clay layers in the polymer matrix. It is particularly interesting to note that the composite morphology exhibits spongy and porous cauliflower-like shape morphology at higher monomer contents in Figure 3(c). This morphological image is well consistent with the previous reports [13, 19, 22].



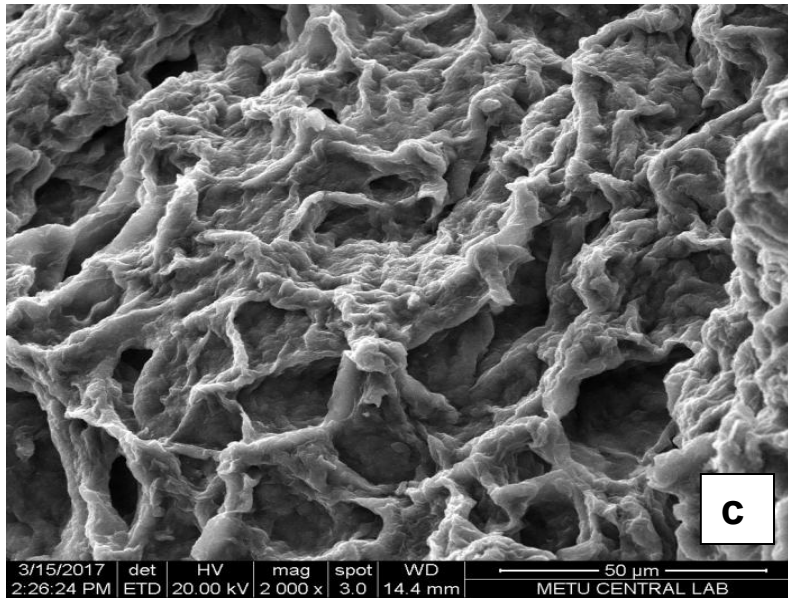


Figure 3. SEM images of (a) Na-MMT, (b) PHMAm/Na-MMT-2 composite, and (c) PHMAm/Na-MMT-4 composite.

Transmission electron microscopy analysis of composites. TEM observations are necessary to determine the morphology of composite and it also provides additional information that will aid in the interpretation of XRD results. The TEM micrograph of PHMAm/Na-MMT-2 composite is shown in Figure 4. The black lines represent the individual MMT layers, while the light areas correspond to the polymer matrix in the micrograph. TEM images of PHMAm/Na-MMT-2 composite show that individual layers of the Na-MMT are well dispersed homogeneously nanoscale in the PHMAm matrix and separated one from the other. Some agglomeration of clay platelets was observed. As shown in Figure 4, the TEM micrograph of PHMAm/Na-MMT-2 composite had layered structure and the individual layers of Na-MMT are well dispersed homogeneously nanometric size in the PHMAm matrix. The circle mark demonstrates intercalated structure. The average particle sizes as evaluated from Figure 4 were varying from 100 to 190 nm. The obtained intercalated structure in PHMAm /Na-MMT-2 composite is good agreement with the XRD result. This feature was similar to the observations of other researchers [23-27].

Determination of antibacterial properties of prepared PHMAm/Na-MMT composites. The antibacterial properties of the PHMAm/Na-MMT composites prepared using *in situ* polymerization were tested using disc diffusion technique [4, 16]. Bacterial strains (*B. cereus* G (+), *S. aureus* G (+), *P. vulgaris* G (-), *P. aeruginosa* G (-), and *E. coli* (35218) G (-)) were screened for their antibacterial activities of composites. Disc diffusion technique was carried out and the zone of inhibition (as millimeters) for different concentrations of composites was measured. Figure 5 shows the inhibition zones that were formed by composite samples. All the inhibition zones measured are also summarized and presented in Table 2.

The results showed that pure Na-MMT exhibited no antibacterial activity when compared with PHMAm/Na-MMT composites. Nevertheless, all the composites exhibited good antibacterial activity and more effective against various pathogens bacterial strain particularly *P. aeruginosa* [Figure 5 (a)]. The antibacterial activity of composites was increased with HMAm monomer content except *E. coli* 35218 G (-) [Figure 5 (b)].

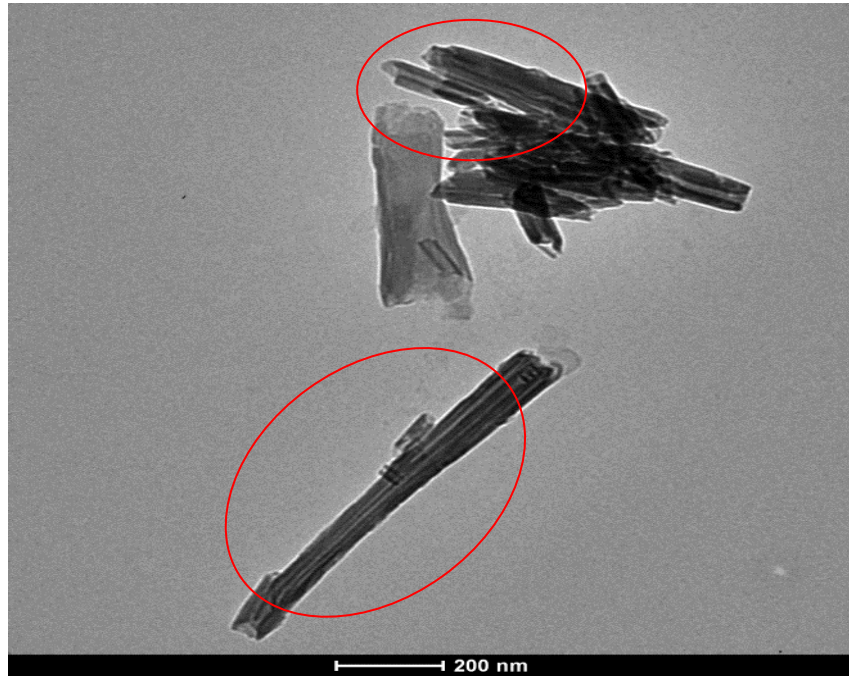


Figure 4. TEM image of PHMAm/Na-MMT-2 composite.

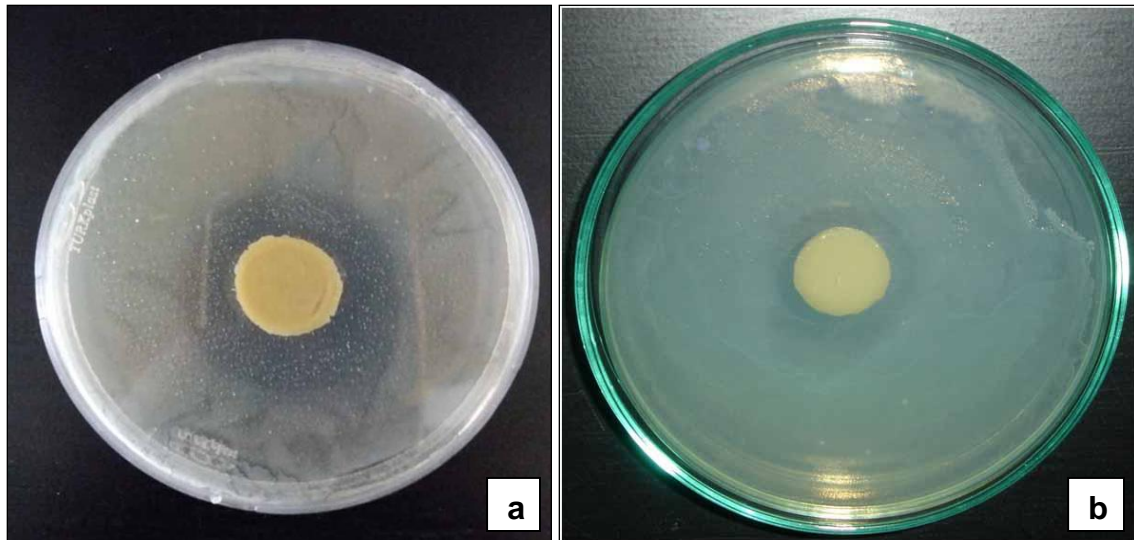


Figure 5. Antibacterial activity results of the PHMAm/Na-MMT3 composites against two pathogenic strains; (a) *P. aeruginosa* G (+) and (b) *E. coli* G (-) shown by the disc diffusion method.

Table 2. Average of inhibition zones obtained from various composites at different concentrations of HMAM^a.

Tested Bacteria	Samples	Average of the inhibition zone (mm)
<i>Bacillus cereus</i> G (+)	Na-MMT	16
	PHMAM / Na-MMT-1	26
	PHMAM / Na-MMT-3	28
<i>Staphylococcus aureus</i> G (+)	Na-MMT	16
	PHMAM / Na-MMT-1	35
	PHMAM / Na-MMT-3	39
<i>Proteus vulgaris</i> G (-)	Na-MMT	16
	PHMAM / Na-MMT-1	30
	PHMAM / Na-MMT-3	36
<i>Pseudomonas aeruginosa</i> G (-)	Na-MMT	16
	PHMAM / Na-MMT-1	40
	PHMAM / Na-MMT-3	45
<i>Escherichia coli</i> (35218) G (-)	Na-MMT	16
	PHMAM / Na-MMT-1	25
	PHMAM / Na-MMT-3	25

^a Diameter of samples is 16 mm before experiment.

CONCLUSION

In this study, PHMAM/Na-MMT composites were synthesized using *in situ* radical polymerization at different contents of HMAM monomer. Intercalated morphology was observed for composites and confirmed by X-ray diffraction results. The scanning electron microscopy revealed that, at a higher content of HMAM, the composite is spongy and porous cauliflower-like shaped morphology and confirmed the dispersion of silicate layers in the PHMAM matrix. TEM image showed the intercalation of PHMAM between the clay layers in nanoscale. The biological activity findings indicated that the antibacterial properties of composites were increased with N-hydroxymethyl acrylamide content except for *E. coli* 35218 G (-).

ACKNOWLEDGEMENT

The authors would like to thank the Ankara University Research Fund for financing and

supporting this project (no. 16L0430012). The authors are grateful to Prof Müşerref Önal for her kind donation of the clay sample.

REFERENCES

1. Çelik, M. and Önal, M. (2006) Preparation and characterization of intercalated poly-methacrylamide/Na-montmorillonite nanocomposites, *JMS Pure App. Chem.*, **A43**, 933-943.
2. Choi, H.J., Kim, J.W., Joo, J. and Kim, B.H. (2001) Synthesis and electrorheology of emulsion intercalated PANI-clay nanocomposite, *Synth. Met.*, **121**, 1325-1326.
3. Anbarasan, R., Arvind, P. and Dhanalakshmi V. (2011) Synthesis and characterization of polymethacrylamide-clay nanocomposites, *J. Appl. Polym. Sci.*, **121**, 563-573.

4. Koç, Z., Çelik, M., Önal, M., Sarıkaya, Y., Öner, Y. and Açık, L. (2014) Study on the synthesis and properties of polyacrylamide/Na-montmorillonite nanocomposites, *J. Compos. Mater.*, **48**, 439-446.
5. Kumar, S., Jog, J.P. and Natarajan, U. (2003) Preparation and characterization of poly(methyl methacrylate)-clay nanocomposites via melt intercalation: the effect of organoclay on the structure and thermal properties, *J. Appl. Polym. Sci.*, **89**, 1186-1194.
6. Koç, Z., Çelik, M., Önal, M., Sarıkaya, Y. and Mogulkoç, Y. (2013) Preparation and characterization of poly(2-hydroxyethyl methacrylate)/Na-montmorillonite intercalated nanocomposites, *J. Polym. Eng.* **33**, 27-32.
7. Herrera-Alonso, J.M, Sedlakova, Z. and Marand, E. (2010) Gas barrier properties of nanocomposites based on *in situ* polymerized poly(*n*-butyl methacrylate) in the presence of surface modified montmorillonite, *J. Membrane Sci.*, **349**, 251-257.
8. Bhiwankar, N. N. and Weiss, R.A. (2006) Melt intercalation/exfoliation of polystyrene-sodium-montmorillonite nanocomposites using sulfonated polystyrene ionomer compatibilizers, *Polym.*, **47**, 6684-6691.
9. Çelik, M. and Önal, M. (2004) Synthesis and characterization of poly(glycidyl methacrylate)/Na-montmorillonite nanocomposites, *J. Appl. Polym. Sci.*, **94**, 1532-1538.
10. Kraisiri D., Chantarasiri N. and Pimpan V. (2012) Thermal behavior of poly(*n*-hydroxymethyl acrylamide) synthesized by inverse emulsion polymerization, *Academic J. Sci.*, **1** (2), 183-188.
11. Önal, M., Sarıkaya, Y., Alemdaroğlu and T. and Bozdoğan, İ. (2003) Isolation and characterization of a smectite as a micro-mesoporous material from a bentonite, *Turk. J. Chem.*, **27**: 683-684.
12. Briesenick, D. and Bremser, W. (2015) Synthesis of polyamide-imide-montmorillonite-nanocomposites via new approach of *in situ* polymerization and solvent casting, *Prog. Org. Coat.*, **82**, 26-32.
13. Çelik, M. and Önal, M. (2012) Synthesis, characterization, and properties of conducting polypyrrole/Na-montmorillonite nanocomposites, *J. Thermoplast. Compos.*, **25**, 505-520.
14. Ramesh, E., Manian, R.D.R.S., Raghunathan, R., Sainath, S. and Raghunathan, M. (2009) Synthesis and antibacterial property of quinolines with potent DNA gyrase activity, *Bioorg. Med. Chem.*, **17**, 660-666.
15. Morsi, R. E., Labena, A. and Khamis, E.A. (2016) Core/shell (ZnO/polyacrylamide) nanocomposite: *In-situ* emulsion polymerization, corrosion inhibition, antimicrobial and anti-biofilm characteristics, *J. Taiwan Inst. Chem. Eng.*, **63**, 512-522.
16. Çelik, M., Qudrat, M.L., Akyüz, E. and Açık, L. (2012) Synthesis and characterization of acrylic fibers-g-polyacrylamide, *Fibers Polym.*, **13**, 145-152.
17. Ghaffari-Moghaddam, M. and Eslahi, H. (2014) Synthesis, characterization and antibacterial properties of a novel nanocomposite based on polyaniline/polyvinyl alcohol/Ag, *Arabian J. Chem.*, **7**, 846-855.
18. Önal, M. and Çelik, M. (2006) Poly-methacrylamide/Na-montmorillonite nanocomposites synthesized by free-radical polymerization, *Mater. Lett.*, **60**, 48-52.
19. Erol Dağ S., Acar Bozkurt P. and Çelik M. (2017) *Journal of the Turkish Chemical Society, Section A: Chemistry*, **4** (sp.is.1), 39-50.
20. Salahuddin, N. and Shehata, M. (2001) Polymethylmethacrylate-montmorillonite composites: preparation, characterization and properties, *Polymer*, **42**, 8379-8385.

21. Tong, X., Zhao, H., Tang, T., Feng, Z. and Huang, B. (2002) Preparation and characterization of poly(ethylacrylate)/bentonite nanocomposites by *in situ* emulsion polymerization, *J. Polym. Sci., Part A: Polym. Chem.*, **40(11)**, 1706-1711.
22. Wang R., Peng, Y., Zhou, M. and Shou, D. (2016) Smart montmorillonite-polypyrrole scaffolds for electro-responsive drug release, *Appl. Clay Sci.*, **134**, 50-54.
23. Kim, S., Park, T.S., Shin, B.C. and Kim, Y.B. (2005) Polymethyl methacrylate/montmorillonite nanocomposite beads through a suspension polymerization-derived process, *J. Appl. Polym. Sci.*, **97**, 2340-2349.
24. Huang, X. and Brittain, W. J. (2001) Synthesis and characterization of pmma nanocomposites by suspension and emulsion polymerization, *Macromolecules*, **34**, 3255-3260.
25. Zhang, X., Xu, R., Wu, Z and Zhou, C. (2003) The synthesis and characterization of polyurethane/ clay nanocomposites, *Polym. Int.*, **52**, 790-794.
26. Li, Y., Zhao, B., Xie, S. and Zhang, S. (2003) Synthesis and properties of poly(methyl methacrylate)/montmorillonite (PMMA/MMT) nanocomposites, *Polym. Int.*, **52**, 892-898.
27. Çelik, M. and Önal, M. (2014) Polythiophene/Na-montmorillonite composites via intercalative polymerization, *J. Thermoplast. Compos.*, **27**, 145-159.